

Self Organization of Tilts in Relay Enhanced Networks: A Distributed Solution

Ali Imran, *Member, IEEE*, Muhammad A. Imran, *Senior Member, IEEE*,
Adnan Abu-Dayya, *Senior Member, IEEE*, and Rahim Tafazolli, *Senior Member, IEEE*

Abstract—Despite years of physical-layer research, the capacity enhancement potential of relays is limited by the additional spectrum required for Base Station (BS)-Relay Station (RS) links. This paper presents a novel distributed solution by exploiting a system level perspective instead. Building on a realistic system model with impromptu RS deployments, we develop an analytical framework for tilt optimization that can dynamically maximize spectral efficiency of both the BS-RS and BS-user links in an online manner. To obtain a distributed self-organizing solution, the large scale system-wide optimization problem is decomposed into local small scale subproblems by applying the design principles of self-organization in biological systems. The local subproblems are non-convex, but having a very small scale, can be solved via standard nonlinear optimization techniques such as sequential quadratic programming. The performance of the developed solution is evaluated through extensive simulations for an LTE-A type system and compared against a number of benchmarks including a centralized solution obtained via brute force, that also gives an upper bound to assess the optimality gap. Results show that the proposed solution can enhance average spectral efficiency by up to 50% compared to fixed tilting, with negligible signaling overheads. The key advantage of the proposed solution is its potential for autonomous and distributed implementation.

Index Terms—Self organization; tilt optimization; relay station; spectral efficiency maximization.

I. INTRODUCTION

THE quest for higher data rates and better quality of service is pushing wireless cellular systems to their physical limits [1]. More extensive use of Relay Stations (RS) has been identified as one of the key strategies to meet the unprecedented high demands in future cellular systems such as LTE-A. Compared to a conventional Base Station (BS), RSs are generally cheaper, more energy efficient and offer a quick roll-out friendly solution to extend the coverage and capacity of cellular systems [2]. However, to exploit the full advantages of RSs, e.g. as intended in LTE-A, two key problems remain challenging to date. The first major problem is to overcome the inherent drawback of RS i.e. the spectrum reuse inefficiency caused by the extra spectrum required for the BS-RS *access link* as illustrated in figure 1. The need for

this extra spectrum severely limits RS' potential of system-wide capacity enhancement in cellular systems [3]. Therefore, it is very desirable to optimize the spectral efficiency of access links so that more spectrum is available for RS-user and BS-user *coverage links*.

Secondly, as identified by 3GPP [4], in future cellular networks such as LTE-A the BS infrastructure that has to support a RS based enhancement, should have Self Organization (SO) capabilities to accommodate the impromptu deployment of the RSs. Such on-the-run random deployment of RSs in time and space is envisioned to be inevitable to cope with spatio-temporally dynamic demands of coverage and capacity in future cellular systems. SO will be particularly required to accommodate advent, departure or location change of RSs. Without proper SO capabilities in BSs, the wide scale deployment of new RSs can be almost as demanding as the deployment of new BSs, thereby severely limiting the advantages of RSs.

The framework presented in this paper addresses both of these challenges simultaneously. i.e. 1) it enhances spectral efficiency on BS-RS access link (without compromising BS-user link spectral efficiency) and thus reduces spectrum reuse inefficiency caused by RSs access links; and 2) it ensures continuous maintenance of the optimal spectral efficiency through a distributed tilt SO solution for BSs to cope with the on-the-run deployment of RSs.

A. Novelty and Contributions

In last decade exhaustive research efforts have been channeled into developing myriad of physical layer [5], MAC layer [6] and network layer [7] solutions to counteract the spectrum reuse inefficiency caused by the access links of RSs. However, remarkably much less attention has been channelled towards solutions that can be harnessed with a system level perspective. In this paper, by exploiting the system level perspective, we present a novel framework for spectral efficiency enhancement of the access link through distributed self-optimization of system-wide BS antenna tilts.

Given the significance of tilt optimization in cellular systems, a large number of works have already embarked on this problem in the context of macro cellular systems [8]–[26]¹. In order to cope with the NP-Hard nature of the problem, these works have mainly resorted to heuristics such as tabu-search [8], fuzzy reinforcement learning [15], fuzzy q-learning

Manuscript received February 17, 2013; revised July 11 and September 23, 2013; accepted November 12, 2013. The associate editor coordinating the review of this paper and approving it for publication was W. Gerstacker.

A. Imran is with the Department of Electrical and Computer Engineering, University of Oklahoma, Tulsa, OK, 74135 USA (e-mail: ali.imran@ou.edu). See www.qson.org for full contact.

A. Abu-Dayya is with Qatar Mobility Innovations Center, Qatar.

M. A. Imran and R. Tafazolli are with the University of Surrey, UK. Digital Object Identifier 10.1109/TWC.2014.011614.130299

¹A detailed survey of works on tilt optimization can be found in our previous work in [27].

[23], golden section search [28], Taguchi method [20], multi-level random Taguchi's method [24], reinforcement learning based sparse sampling [25] and simulated annealing [26]. The general methodology followed in these works has been to evaluate the desired Key Performance Indicator(s) (KPIs) as a function of system-wide tilt angles through a simulation model. A non-exhaustive search for the suitable tilt values is then carried out by exploration of the solution space in vicinities selected with help of one of the aforementioned heuristics. Given the limited transparency of the simulation models that act as a black box between the tilt value and the KPI, the quality of the solution yielded by this methodology remains hard to be assessed. The inherent lack of assurance from these heuristics that the solution produced is close to optimal is another disadvantage. Furthermore, the long time required to search for an acceptable system-wide solution using this approach relying on sophisticated offline planning tools is another factor that thwarts the practical implementation of such solutions for self organising antenna tilts in an online manner. No repeatability and no convergence guarantee is another hurdle in the use of this approach for self organization of tilts in live networks. To overcome these challenges, in this paper we exploit a mathematical framework to model the KPI of interest as a function of tilt, thereby obtaining a more transparent system model that allows deeper insights and thus better control of system behaviour. Then, instead of solving for the system-wide NP-hard problem through a heuristic, we propose to decompose the problem into local sub-problems that, because of being of very small scale, can be solved by more deterministic methods and thus can have better quality assurance.

Another novelty of our work is that prior works have mainly focused on tilt optimization in macro cellular systems and do not consider relay enhanced cellular systems with consideration of BS-RS access links, as we do in this work. Only in [29] have authors introduced the concept of spectral efficiency enhancement on access link through BS antenna tilt adaptation for the first time. However, the scope of [29] is limited to an ideally symmetric scenario where all the cells are assumed to contain strictly one RS in each cell. Thus, it does not take into account more generic scenarios of heterogeneous deployment where RSs are deployed quite randomly and some cells might not contain RSs and some users are directly served by BSs. The gain of the solution proposed in [29] is demonstrated with a model consisting of only three cells whereas we conduct performance evaluation using a full scale system model. Also, while considering BS-RS link, the solution in [29] does not take into account the impact of BS antenna tilting on the BS-user links, as we do in this work. Therefore, to the best of our knowledge, this paper presents a novel distributed solution for run-time self optimization of system-wide tilts in relay enhanced cellular systems with realistic heterogeneous deployments. We compare the performance of our proposed solution with three different benchmarks. 1) Performance with no tilting in the system 2) Performance with a range of pragmatic fixed tilting values that are generally used in state of the art commercial cellular networks. This includes fixed optimal tilt values depending on cell size and antenna height 3) Performance with a globally

optimal centralized SO solution obtained for a small scale version of the problem through a brute force method. The key advantage of the proposed solution is that it can enhance average BS-RS as well as BS-user link spectral efficiency while dynamically coping with run time addition of relays in the system without requiring centralized signalling and manual reconfiguration of BS antenna tilts.

B. Organization of paper

The rest of paper is organized as follows: in section II we present the system model, assumptions and problem formulation. In order to achieve a SO solution, in section III we propose a way to decompose the system-wide problem into local subproblems as inspired by SO systems in nature. The solution methodology for local subproblems is also presented in this section. Section IV presents numerical as well as system level simulation results to demonstrate the gains achievable by the proposed solution. Pragmatic implementation of the proposed solution in the context of LTE-A is given in section V and section VI concludes this paper.

II. SYSTEM MODEL AND ASSUMPTIONS

A. Assumptions and Nomenclature

The analysis in this paper only focuses on the *downlink* of cellular systems for the sake of conciseness. It is assumed that all user devices and RSs have omnidirectional antennas with a constant gain in all directions. The term sector is used with the same meanings as a cell. Frequency reuse of one is considered and consequently we assume an interference limited scenario where noise is negligible compared to interference. Since, the time scale of self optimization of tilts will be in the order of hours to days, short term channel variations, i.e. fast fading, are omitted in the analytical model for better tractability. However, the features omitted in the analysis, namely noise and fast fading, are modeled in detail in the simulation model used for performance evaluation in Section IV to assess the performance of the proposed solution in more realistic scenarios. We use the term throughput in this paper with similar meaning as the bandwidth normalized ergodic capacity given by $\log_2(1+SIR)$ that is thus equivalent to the *spectral efficiency* in b/s/Hz, where SIR stands for Signal to Interference Ratio. BS and RS are multiplexed in time (or frequency) such that there is no interference between RS-user and BS-RS links as illustrated in figure 1. Due to the geometrical context of the paper, while referring to BS, RS and users we will be referring to the locations of their antennas unless specified otherwise. The symbol *tilde*, e.g. in \tilde{x} , is used to denote the optimal value of a variable x and the symbol *hat*, e.g. in \hat{x} , is used to denote an approximation of a variable x .

B. System Model

We consider a sectorized multi cellular network as shown in figure 2. Each BS has three cells and each cell has at most one RS station placed at an arbitrary location. The purpose of the RS can be to cover a random user hotspot for capacity enhancement or to fill a coverage hole for coverage enhancement. Let \mathcal{B} denote the set of points corresponding to

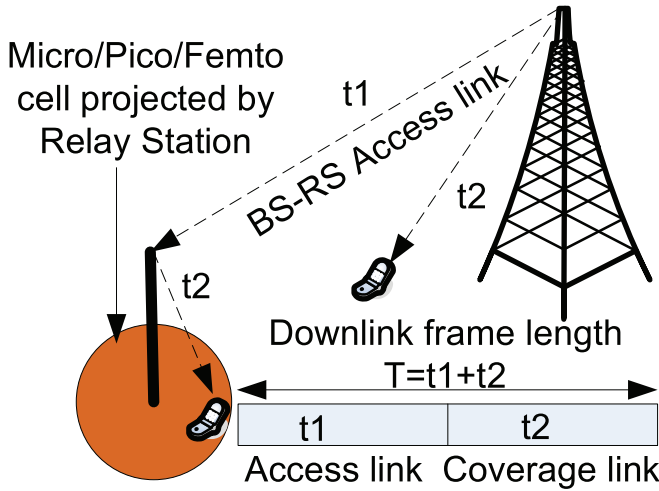


Fig. 1. The extra spectrum required for an access link causes spectrum reuse inefficiency. This inefficiency can be decreased by maximising the spectral efficiency on access link as that will allow a reduction in t_1 and an increase in t_2 .

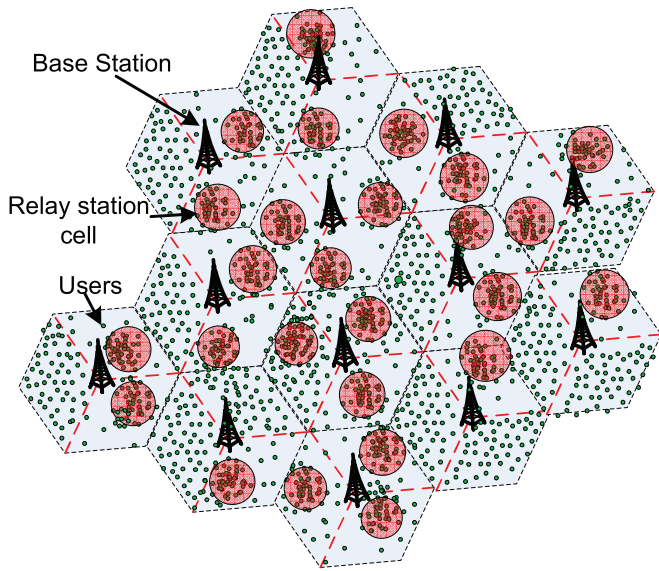


Fig. 2. System model for problem formulation. Small (red) circles show RS that are randomly located in some sectors to cover hotspots etc.

the transmission antenna location of all BS cells, \mathcal{R} denote the set of points representing locations of the RSs antennas in the system and \mathcal{U} denote set of points representing all the user devices randomly located in the system. The geometric SIR on the access link of a RS located at point $r \in \mathcal{R}$ associated with b^{th} BS cell can be given as:

$$\gamma_r^b = \frac{P^b G_r^b G_r \delta_r^\alpha (d_r^b)^{-\beta}}{\sum_{v \in \mathcal{B} \setminus b} (P^v G_r^v G_r \delta_r^\alpha (d_r^v)^{-\beta})} \quad b, v \in \mathcal{B}, r \in \mathcal{R} \quad (1)$$

where P^b is the transmission power of the b^{th} BS cell, d_r^b and d_r^v are the distances between the b^{th} and v^{th} BS cell (transmitting) antenna locations and (receiving) RS antenna location r . α and β are pathloss coefficient and exponents respectively that can be used to model a generic pathloss model. δ_r^b and δ_r^v are shadowing coefficients that represent

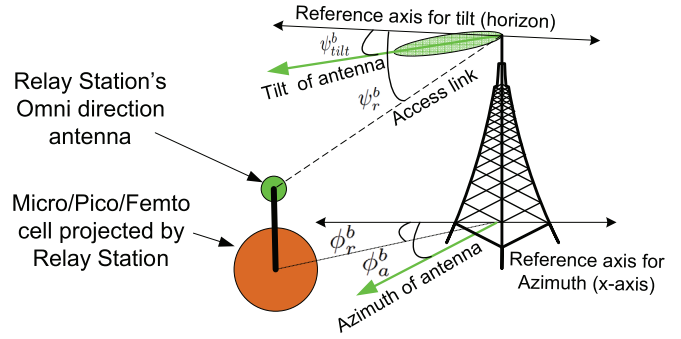


Fig. 3. Illustration of geometrical background of the analysis.

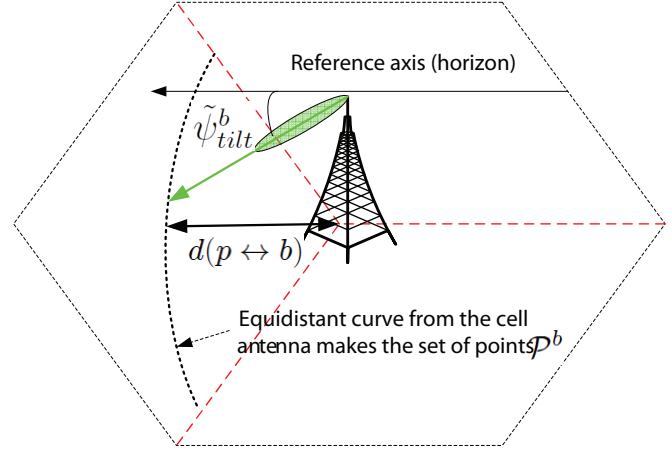


Fig. 4. The optimal tilt $\tilde{\psi}_{tilt}^b$ can be mapped to a locus of points equidistant distant from the BS.

shadowing faced by a signal at location r while being received from the b^{th} and \tilde{b}^{th} BS antennas, respectively. Note that δ_r^b and $\delta_r^{\tilde{b}}$ are not assumed to be same, despite being shadowing values at same location. This is because, in order to model a more realistic propagation scenario, we take into account the dependency of shadowing values on the angles of arrival, using the multi-cell cross-correlation shadowing model proposed in [30]. The operator ' \setminus ' in $\mathcal{B} \setminus b$ means all elements of \mathcal{B} except b .

G_r^b and $G_r^{\tilde{b}}$ are antenna gains perceived at the r^{th} RS from b^{th} and \tilde{b}^{th} BS respectively. For 3GPP LTE the three dimensional antenna pattern can be modelled as proposed in [31]. Using the geometry in figure 3 the perceived antenna gain from the b^{th} BS, at location r of a RS can be written as (2) where ψ_r^b is the vertical angle at the b^{th} cell in degrees from the reference axis (horizon) to the RS r . ψ_{tilt}^b is the tilt angle of the b^{th} cell as shown in figure 3. ϕ_a^b is the angle of the azimuth orientation of the antenna with respect to the horizontal reference axis i.e. positive x-axis. ϕ_r^b is the angle of location r^{th} RS from the horizontal reference axis, at the b^{th} BS. Subscripts h, a and v denote horizontal, azimuth and vertical respectively. Thus B_h and B_v represent horizontal and vertical beamwidths of the BS antenna respectively, and λ_h and λ_v represent weighting factors for the horizontal and vertical beam pattern of the antenna in the 3D antenna model [31] respectively. G_{max} and A_{max} denote the maximum antenna gain at the boresight of the antenna and maximum antenna attenuation at the sides and back of the boresight of

$$G_r^b = 10^{0.1 \left(\lambda_v \left(G_{max} - \min \left(12 \left(\frac{\psi_r^b - \psi_{tilt}^b}{B_v} \right)^2, A_{max} \right) \right) + \lambda_h \left(G_{max} - \min \left(12 \left(\frac{\phi_r^b - \phi_a^b}{B_h} \right)^2, A_{max} \right) \right) \right)} \quad (2)$$

the antenna respectively, in dB. G_{max} and A_{max} are the same for the horizontal and vertical radiation pattern, therefore, no subscript v and h are associated with them.

In order to substitute in (8), in (2) the antenna model can be simplified by neglecting the maximum attenuation factor A_{max} and assuming the maximum gain G_{max} as 0 dB. Both of these assumptions preserve the required accuracy of this antenna model i.e. the parabolic dependency of antenna gain on the angular distance from the boresight stays unchanged. At the same time these assumptions allow the analytical tractability and insights that otherwise would not be possible. *Nevertheless, these assumptions will be removed in the simulation and numerical analysis presented in Section IV. Therefore the results presented in this paper depict the performance of the proposed solution in a system model without these simplifications.* The simplified antenna model can be written as:

$$G_r^b = 10^{-1.2 \left(\lambda_v \left(\frac{\psi_r^b - \psi_{tilt}^b}{B_v} \right)^2 + \lambda_h \left(\frac{\phi_r^b - \phi_a^b}{B_h} \right)^2 \right)} \quad (3)$$

We assume that all the base stations transmit with the same power and all RS antennas have constant gain in all directions i.e. $G_r = \text{constant}$. Thus, by using (3) in (1) the SIR on the access link of the r^{th} RS can be determined as (4). For the ease of expression we use following substitutions:

$$c_k^b = \frac{B_v^2 \lambda_h}{\lambda_v} \left(\frac{\phi_r^b - \phi_a^b}{B_h} \right)^2 ; \quad c_k^b = \frac{B_v^2 \lambda_h}{\lambda_v} \left(\frac{\phi_r^b - \phi_a^b}{B_h} \right)^2 \quad (5)$$

$$h_r^b = \delta_r^b \alpha (d_r^b)^{-\beta} ; \quad h_r^b = \delta_r^b \alpha (d_r^b)^{-\beta} ; \quad \mu = \frac{-1.2 \lambda_v}{B_v^2} \quad (6)$$

Using the substitutions in (5)–(6), the SIR in (4) can be written as:

$$\gamma_r^b = \frac{h_r^b 10^{\mu \left((\psi_r^b - \psi_{tilt}^b)^2 + c_r^b \right)}}{\sum_{\forall b \in \mathcal{B}} \left(h_r^b 10^{\mu \left((\psi_r^b - \psi_{tilt}^b)^2 + c_r^b \right)} \right)} \quad (7)$$

Note that γ_r^b is a function of the vector of tilt angles of all sectors i.e. $\psi_{tilt}^B = [\psi_{tilt}^1, \psi_{tilt}^2, \psi_{tilt}^3 \dots \psi_{tilt}^B]$ where $B = |\mathcal{B}|$, but for the sake of simplicity of expression we will show this dependency only where necessary. Similarly the geometric SIR perceived by a user at a location u being served by the b^{th} BS cell can be given as:

$$\gamma_u^b = \frac{P^b G_u^b \alpha (d_u^b)^{-\beta}}{\sum_{\forall b \in \mathcal{B} \setminus b} \left(P^b G_u^b \alpha (d_u^b)^{-\beta} \right)} \quad b, \hat{b} \in \mathcal{B}, u \in \mathcal{U} \quad (8)$$

where d_u^b and $d_u^{\hat{b}}$ are distances between the b^{th} and \hat{b}^{th} BS cell and u^{th} user. Following the same steps as above, the SIR for the BS-user link can be written as:

$$\gamma_u^b = \frac{h_u^b 10^{\mu \left((\psi_u^b - \psi_{tilt}^b)^2 + c_u^b \right)}}{\sum_{\forall b \in \mathcal{B} \setminus b} \left(h_u^b 10^{\mu \left((\psi_u^b - \psi_{tilt}^b)^2 + c_u^b \right)} \right)} \quad (9)$$

III. TILT OPTIMIZATION FRAMEWORK

In this section, first the problem is formulated using the system model. Key steps to design a SO solution are identified by inspirations from natural SO systems. These steps are then applied to our system model to design the analytical framework for a SO solution.

A. Problem Formulation

Our objective is to minimize the radio resources required for the access link and thus maximize the net gain of RSs in terms of system-wide capacity. To achieve this objective, we propose to optimize system-wide BS antenna tilts such that it maximizes the long term weighted average bandwidth normalized throughput η i.e. weighted average spectral efficiency (bandwidth normalized ergodic capacity) on all the access links in the system. Mathematically our problem can be written as:

$$\max_{\psi_{tilt}^B} \eta (\psi_{tilt}^B) = \max_{\psi_{tilt}^B} \frac{1}{W_r} \sum_{\forall r \in \mathcal{R}} w_r \log_2 (1 + \gamma_r^b (\psi_{tilt}^B)) \quad (10)$$

where $0 < w_r \leq 1$ is a weight factor that varies over a fixed range of 0-1 and can be assigned to each RS to reflect the relative importance of its backhaul link in overall system level optimization. In other words, these weights can be set to model the significance of each RS depending on statistics of the number and activity levels of users it serves. Thus these weights can also be used to reflect if a RS has been deployed for coverage extension and therefore might have low load backhaul that needs to be assigned a lower weight. In case the RS is for capacity extension at a hotspot it might have a heavily loaded backhaul that needs to be assigned proportionally higher w_r . Where, $W_r = \sum_{\forall r \in \mathcal{R}} w_r$. In a simple example, w_r can be calculated as follows:

$$w_r = \frac{\sum_{\forall u \in \mathcal{U}_b^r} a_u}{\sum_{\forall u \in \mathcal{U}_b} a_u} , \quad 0 < a_u \leq 1 \quad (11)$$

Where a_u represents u^{th} user activity level. \mathcal{U}_b is set of users in the b^{th} BS cell and \mathcal{U}_b^r is set of users in the r^{th} RS cell within b^{th} BS cell. However, adapting BS antenna tilt will have an impact on the users that are directly served by BS.

To take these users into account the problem in (10) can be reformulated as (12) where $\hat{\mathcal{U}}$ is the set of users served by the RSs such that $\hat{\mathcal{U}} \subset \mathcal{U}$ and thus users served directly by the BS are given by set $\mathcal{U} \setminus \hat{\mathcal{U}}$ and $\hat{A}_u = \sum_{\forall u \in \mathcal{U} \setminus \hat{\mathcal{U}}} a_u$.

The formulation in (12) is a nonlinear multi variable optimization problem. Its solution would require global cooperation among all cells in the system and hence cannot be implemented as a distributed SO solution [27], [32]. Furthermore, as we will see in subsection III-E the objective function in (12) is non-convex. Also, the huge number of optimization variables i.e. $\psi_{tilt}^B = [\psi_{tilt}^1, \psi_{tilt}^2, \psi_{tilt}^3 \dots \psi_{tilt}^B]$, mean it is a large scale optimization problem. Therefore, the conventional heuristic based approach of finding a sub-optimal solution by using

$$\gamma_r^b = \frac{\delta_r^b \alpha (d_r^b)^{-\beta} 10^{-1.2 \left(\lambda_v \left(\frac{\psi_r^b - \psi_{tilt}^b}{B_v} \right)^2 + \lambda_h \left(\frac{\phi_r^b - \phi_{tilt}^b}{B_h} \right)^2 \right)}}{\sum_{\forall b \in \mathcal{B} \setminus b} \left(\delta_r^b \alpha (d_r^b)^{-\beta} 10^{-1.2 \left(\lambda_v \left(\frac{\psi_r^b - \psi_{tilt}^b}{B_v} \right)^2 + \lambda_h \left(\frac{\phi_r^b - \phi_{tilt}^b}{B_h} \right)^2 \right)} \right)} \quad (4)$$

$$\max_{\psi_{tilt}^B} \left(\frac{1}{W_r} \sum_{\forall r \in \mathcal{R}} w_r \log_2 (1 + \gamma_r^b (\psi_{tilt}^B)) + \frac{1}{A_u} \sum_{\forall u \in \mathcal{U} \setminus u} a_u \log_2 (1 + \gamma_u^b (\psi_{tilt}^B)) \right) \quad (12)$$

offline planning tools, does not offer a pragmatic mechanism for online self optimization of tilts due to the very large computational time. Furthermore, the lack of guarantee of the quality of the solution and limitations of the offline planning tool to depict the live network may not only compromise the agility of the closed loop nature of an ideal SO solution but also may increase instability risks in the SO process [27]. In the following section we present a novel biologically inspired mathematical framework that can enable self optimization of tilts by providing a distributed solution of (12).

B. Designing a Self Organizing Solution

In nature many systems can be observed which exhibit self organizing behaviour. A detailed discussion on designing self organization by mimicking such systems can be found in our works in [27], [33] as well as in [32], [34], [35]. Here it would suffice to say that, for a distributed self organizing solution, a perfect objective may not be aimed for at system-wide level [32]. Rather, an approximation of the objective can be aimed for, given that it can be decomposed into sub-objectives that can be achieved at local level while requiring interactions only among local entities of the system. This phenomenon, in turn, can approximately achieve the original system wide objective resulting in the emergence of self organizing behaviour [27], [32].

This design principle of SO, when applied to our problem in (12), means that given the complexity of this problem, we need to 1) find an alternative approximate manifestation of the problem in (12) that can be then 2) decomposed down into easily solvable local sub-problems whose solution will at most require local coordination only among neighbouring cells. And finally we need to 3) determine the solution of those local subproblems. In the next three subsections we follow these three steps to achieve a distributed self organising solution for the problem in (12).

C. Simplifying the Problem to Achieve Decomposability

The difficulty to obtain a pragmatic solution of (12) stems mainly from the fact that there is a summation in the optimization objective that grows with the number of users. The complexity of each term in the summation also grows with the number of cells in the system. In the following we present the analysis to determine a significantly simpler and scalable manifestation of (12) as desired for the distributed SO solution.

Theorem 1. *If a cell has uniform user distribution and the importance of each geographical point (x,y) in the cell is given by weight $a_{(x,y)}$, the antenna tilt $\tilde{\psi}_{tilt}^b$ of that cell is optimal in terms of weighted average area spectral efficiency if it satisfies following condition:*

$$\int_x \int_y a_{(x,y)} \left((\psi_{x,y}^b - \tilde{\psi}_{tilt}^b) \frac{\tilde{\gamma}_{x,y}^b}{1 + \tilde{\gamma}_{x,y}^b} \right) dx dy = 0 \quad (13)$$

where $\tilde{\gamma}_{x,y}^b$ is the SIR perceived at point (x,y) in cell b , when its antenna is tilted by $\tilde{\psi}_{tilt}^b$ degrees. $\tilde{\gamma}_{x,y}^b$ can be given as (14) The integral in (13) is a surface integral over the whole area of the cell projected by the BS antenna at location b and (x,y) denote the coordinate of an arbitrary point in that cell.

Proof: Proof of theorem 1 is provided in Appendix A ■

The following corollaries can be deduced from theorem 1:

Corollary 1. *If the tilt value for a given cell satisfies the condition:*

$$\sum_{u=1}^{|\mathcal{U}_b|} a_u \left((\psi_u^b - \tilde{\psi}_{tilt}^b) \frac{\tilde{\gamma}_u^b}{1 + \tilde{\gamma}_u^b} \right) = 0 \quad (15)$$

it will yield greater or equal weighted average spectral efficiency on BS-user links than that obtained with any other value of tilt, for the same tilt angles of neighbouring cells. Mathematically it can be expressed as (16) where \mathcal{U}_b is set of users in the b^{th} cell and $A_u^b = \sum_{\forall u \in \mathcal{U}_b} a_u$. Note that $\tilde{\gamma}_u^b$ here is function of antenna tilt of the b^{th} cell only, as rest of the antenna tilts are fixed.

Proof: Proof of corollary 1 directly follows proof of theorem 1 when generalized for a arbitrary user distribution whether uniform or non-uniform; and arbitrary user activity levels whether homogeneous or non-homogenous. (see result (52) in Appendix A) ■

Corollary 2. *If H^b and H^p are the heights of the b^{th} cell antenna and point p and $d(p \leftrightarrow b)$ denotes the distance between the b^{th} BS and a user at point p ; then the optimal tilt angle in that cell $\tilde{\psi}_{tilt}^b$ is the tilt that optimizes spectral efficiency at the point p that belongs to a set of points \mathcal{P}^b such that $\mathcal{P}^b = \{p | d(p \leftrightarrow b) = d^b\}$ and $d^b = (H^b - H^p) / \tan(\tilde{\psi}_{tilt}^b)$.*

Proof: This corollary follows theorem 1 through the fact that the optimal tilt angle $\tilde{\psi}_{tilt}^b$ given by theorem 1 can be transformed into a locus of points \mathcal{P}^b that lie at distance d^b from the b^{th} cell antenna. This is illustrated in figure 4. ■

$$\tilde{\gamma}_{x,y}^b = \frac{d_{x,y}^b \cdot 10^{-\beta} \cdot 10^{-1.2 \left(\lambda_v \left(\frac{\psi_{x,y}^b - \tilde{\psi}_{tilt}^b}{B_v} \right)^2 + \lambda_h \left(\frac{\phi_{x,y}^b - \phi_{tilt}^b}{B_h} \right)^2 \right)}}{\sum_{\forall b \in \mathcal{B} \setminus b} \left(d_{x,y}^b \cdot 10^{-\beta} \cdot 10^{-1.2 \left(\lambda_v \left(\frac{\psi_{x,y}^b - \tilde{\psi}_{tilt}^b}{B_v} \right)^2 + \lambda_h \left(\frac{\phi_{x,y}^b - \phi_{tilt}^b}{B_h} \right)^2 \right)} \right)} \quad (14)$$

$$\frac{1}{A_u} \sum_{\forall u \in \mathcal{U}_b} a_u \log_2(1 + \gamma_u^b(\tilde{\psi}_{tilt}^b)) \geq \frac{1}{A_u} \sum_{\forall u \in \mathcal{U}_b} a_u \log_2(1 + \gamma_u^b(\psi_{tilt}^b)) \quad \forall 0 \leq \psi_{tilt}^b \leq 90 \quad (16)$$

Note that according to theorem 1 and its subsequent corollaries, a tilt angle of the b^{th} cell optimized for any of the points in set \mathcal{P}^b , optimizes the average spectral efficiency in that cell. In other words set \mathcal{P}^b represents the set of focal points with respect to which the tilt should be maximized in a given cell with given user distribution and given user activity levels. However, in order to consider the impact of interference from neighbouring cells and jointly optimize tilts, a single focal point in \mathcal{P}^b needs to be identified that can represent the user distribution in the b^{th} cell. Note that theorem 1 and subsequent corollaries have effectively reduced the search space for this single point from the whole cell area to a small set of points given by \mathcal{P}^b . Now, for any given user distribution in a cell this single focal point $p^b \in \mathcal{P}^b$ can be determined by invoking the classic definition of centre of gravity of a two dimensional mass distribution with an additional simplification that the CG lies within \mathcal{P}^b , as follows:

$$\tilde{p}^b = \arg \min_{\mathcal{P}^b} \sum_{\forall u \in \mathcal{U}_b} a_u d_u^p(p^b \leftrightarrow u) \quad (17)$$

For ease of discussion, we refer to this focal point as Center of Gravity (CG) of a cell for its given user distribution and user activity profile. Fortunately, as long as the user distribution and activity can be assumed uniform across the cell, CG can be shown to lie at the centroid of the trapezoid that constitutes the sector. In such a case CG can be determined based on cell size and antenna heights without having to take into account user distribution and activity profile.

Using theorem 1 and its corollaries, the users distribution in each cell can be represented by a single focal point for the tilt optimization process for an arbitrary user distribution and user activity profile. If the collection of all such points in the system is given by the set \mathcal{V} it can be defined as $\mathcal{V} = \bigcup_{\forall b \in \mathcal{B}} \tilde{p}^b$ where $\tilde{p}^b \in \mathcal{P}^b$. By using this definition of \mathcal{V} in conjunction with corollary 1 and 2, the 2^{nd} summation of the right hand side of the optimization problem in (12) can be written as (18) where $\check{\mathcal{V}}$ and $\tilde{\mathcal{V}}$ are sets of CGs representing BS associated users in cells with RS and without RS respectively, such that $\mathcal{V} = \{\check{\mathcal{V}} \cup \tilde{\mathcal{V}}\}$. Substituting (18) in (12) we get (19). To further simplify our optimization problem in (19) we propose the following generic method to determine a single point s_b that can represent the effective CG in each cell for the purpose of tilt optimization, including the cells that contain coverage

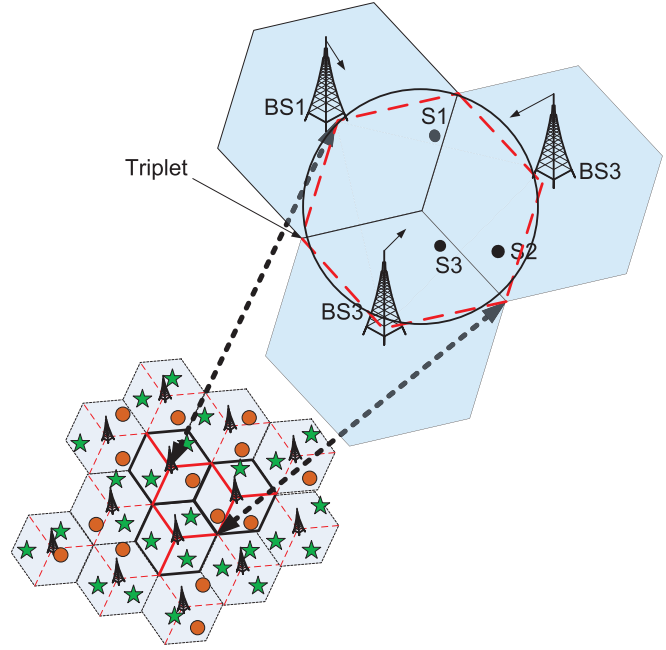


Fig. 5. Circles represent points in set \mathcal{R} i.e., RS locations and stars represent points in set \mathcal{V} i.e. focal points of user distributions in a cell determined through theorem (1) and its corollaries. Stars and circles together make set \mathcal{S}

or capacity enhancing RSs:

$$s_b = \begin{cases} r_b, & \text{if } |\mathcal{U}_b^r| > 0 \ \& \ w_r \geq \frac{\sum_{\forall u \in \mathcal{U}_b^b} a_u}{\sum_{\forall u \in \mathcal{U}_b} a_u}, \text{ where } r_b \in \mathcal{R} \\ \check{v}_b, & \text{if } |\mathcal{U}_b^r| > 0 \ \& \ w_r < \frac{\sum_{\forall u \in \mathcal{U}_b^b} a_u}{\sum_{\forall u \in \mathcal{U}_b} a_u}, \text{ where } \check{v} \in \check{\mathcal{V}} \\ \tilde{v}_b, & \text{otherwise, where } \tilde{v} \in \tilde{\mathcal{V}} \end{cases} \quad (20)$$

where \mathcal{U}_b^b denotes the set of users in the b^{th} cell that are directly associated with the BS. Thus case 1 of (20) refers to the scenario where the RS is serving the majority of users and thus is expected to have a capacity limited backhaul link that must be considered in the tilt optimization process. This case is applicable to capacity enhancing RS installed at hotspots in a cell. The second case of (20) represents the cells where the main purpose of the RS is coverage extension. The backhaul of such RS is not expected to be capacity limited and therefore does not have to be considered directly in the tilt optimization problem. In this case the CG of the respective cell will be determined by the users associated directly with the BS. The third case of equation (20) represents the cells with no RSs. Now if we define \mathcal{S} as set of all points s_b in the system such that $|\mathcal{S}| = |\mathcal{B}|$, based on arguments presented above through

$$\frac{1}{A_u} \sum_{\forall u \in \mathcal{U} \setminus \mathcal{U}} a_u \log_2(1 + \gamma_u^b(\psi_{tilt}^B)) \equiv \sum_{\forall v \in \mathcal{V}} \log_2(1 + \gamma_v^b(\psi_{tilt}^B)) + \sum_{\forall v \in \mathcal{V}} \log_2(1 + \gamma_v^b(\psi_{tilt}^B)) \quad (18)$$

$$\max_{\psi_{tilt}^B} \left(\frac{1}{W_r} \sum_{\forall r \in \mathcal{R}} w_r \log_2(1 + \gamma_r^b(\psi_{tilt}^B)) + \sum_{\forall \check{v} \in \mathcal{V}} \log_2(1 + \gamma_{\check{v}}^b(\psi_{tilt}^B)) + \sum_{\forall \check{v} \in \mathcal{V}} \log_2(1 + \gamma_{\check{v}}^b(\psi_{tilt}^B)) \right) \quad (19)$$

(13)–(20), the problem in (19) can be written as:

$$\max_{\psi_{tilt}^B} \zeta(\psi_{tilt}^B) = \max_{\psi_{tilt}^B} \sum_{\forall s \in \mathcal{S}} \log_2(1 + \gamma_s^b(\psi_{tilt}^B)) \quad (21)$$

The points (CGs) in set \mathcal{S} are shown in figure 5, where circles represent RSs i.e. points in set \mathcal{R} ; and stars represent the CGs of users' geographical distribution in cells with no RS or with RS whose backhaul is not critical for the optimization process i.e. RS with $w_r < \frac{\sum_{\forall u \in \mathcal{U}_b^a} a_u}{\sum_{\forall u \in \mathcal{U}_b} a_u}$. Note that $|\mathcal{S}| \ll |\mathcal{U} \setminus \mathcal{U} \cup \mathcal{R}|$. Thus, as highlighted in section III-B, for designing a SO solution, (21) is the required simplified manifestation of the original problem in (12).

D. Decomposing the Simplified Problem into Subproblems

As discussed in section III-B, for a distributed SO solution, after simplifying the original problem in (12) into (21) its decomposition into local subproblems is required to transform it from a large scale optimization problem to a small scale optimization problem. Such decomposition into local subproblems is common in SO systems in nature as explained via a case study of the flock of common cranes above (see [36] and [33] for details). We refer to the same case study and deduce the fact that, for achieving the flock-wide objective of flying in V-formation, each crane merely relies on the observation of its two immediate neighbours, one on each side. Thus, although cranes do not achieve and maintain a perfect V formation, they can still achieve up to 70% gain in group flight efficiency [36]. To exploit the same principle in our problem, we compromise slightly on global optimization of the problem and propose a concept of a *triplet* to enable its local decomposition. A triplet consists of three immediate neighbour cells as illustrated in the enlarged part of figure 5. Its use is explained and justified by the following rather intuitive arguments:

Lemma 1. *The average spectral efficiency at the CG's in the system when interference from only two immediate neighbouring sectors is considered, will be greater than or equal to the average spectral efficiency at the same points when interference from all the sectors is considered. Mathematically $\hat{\zeta} \geq \zeta$: where*

$$\hat{\zeta} = \frac{1}{|\mathcal{S}|} \sum_{\forall s \in \mathcal{S}} \log_2(1 + \hat{\gamma}_s^b(\psi_{tilt}^{\hat{B}})) \quad (22)$$

and

$$\hat{\gamma}_s^b(\psi_{tilt}^{\hat{B}}) = \frac{h_s^b 10^{\mu((\psi_s^b - \psi_{tilt}^b)^2 + c_s^b)}}{\sum_{\forall \check{b} \in \hat{B} \setminus b} (h_s^{\check{b}} 10^{\mu((\psi_s^{\check{b}} - \psi_{tilt}^{\check{b}})^2 + c_s^{\check{b}})})}, b, \check{b} \in \hat{B}, \quad (23)$$

where $\hat{B} \subset \mathcal{B}$ and b here represents the antenna location of an arbitrary cell in which point s lies and \hat{B} is the set of b^{th} and the two other most interfering cells adjacent to the b^{th} sector all mutually facing each other such that $|\hat{B}| = \hat{B} = 3$. The set of three cells represented by \hat{B} are termed as a triplet as illustrated in figure 5 by dashed red lines. $\psi_{tilt}^{\hat{B}}$ is the vector of tilt angles of \hat{B} sectors within the triplet.

Proof: Proof of Lemma 1 is provided in Appendix B ■

Corollary 3. *As β and the cell radius grow large, $\hat{\zeta}$ becomes a closer approximation of ζ*

Proof: Corollary 3 can be easily proved by putting large values of β and d in (55). ■

Proposition 1. *If the SIR is given by $\hat{\gamma}_s^b$, the maximum aggregate throughput achieved in the system by optimizing the tilts within each triplet independently, is the same as the throughput achieved by optimizing system-wide tilts. Mathematically, $\hat{\zeta}_{N,max} = \hat{\zeta}_{max}$, where*

$$\hat{\zeta}_{max} = \max_{\psi_{tilt}^B} \hat{\zeta}(\psi_{tilt}^B) = \max_{\psi_{tilt}^B} \sum_{\forall s \in \mathcal{S}} \log_2(1 + \hat{\gamma}_s^b) \quad (24)$$

where $\hat{\gamma}_s^b$ is the approximate SIR at point s given by (23) and

$$\hat{\zeta}_{N,max} = \sum_{\forall n \in \mathcal{N}} \hat{\zeta}_{n,max} \quad (25)$$

where

$$\hat{\zeta}_{n,max} = \max_{\psi_{tilt}^{\mathcal{T}_n}} \sum_{\forall s \in \mathcal{S}_n} \log_2(1 + \hat{\gamma}_s^b(\psi_{tilt}^{\mathcal{T}_n})) \quad (26)$$

where $\mathcal{S}_n \subset \mathcal{S}$, $\mathcal{T}_n \subset \mathcal{N}$, $\forall n \in \mathcal{N}$ and \mathcal{T}_n is the n^{th} triplet as illustrated in figure 5 and $|\mathcal{S}_n| = |\mathcal{T}_n| = T_n = 3$, $\forall n \in \mathcal{N}$, $\psi_{tilt}^{\mathcal{T}_n}$ is the vector of tilt angles of sectors within n^{th} triplet such that

$$\mathcal{S}_n \cap \mathcal{S}_{\hat{n}} = \Phi \text{ and } \mathcal{T}_n \cap \mathcal{T}_{\hat{n}} = \Phi, \forall n \neq \hat{n} \text{ where } n, \hat{n} \in \mathcal{N} \quad (27)$$

\mathcal{N} is the set of all such triplets, such that $|\mathcal{N}| = \frac{|\mathcal{B}|}{|\mathcal{T}_n|}$ is the total number of triplets in the system.

Proof: Since $|\mathcal{N}| \times |\mathcal{T}_n| = |\mathcal{N}| \times |\mathcal{S}_n| = |\mathcal{B}| = |\mathcal{S}|$ so (24) can be written as:

$$\begin{aligned} \hat{\zeta}_{max} = \max_{\psi_{tilt}^B} \{ & \sum_{\forall s \in \mathcal{S}_1} \log_2(1 + \hat{\gamma}_s^b(\psi_{tilt}^{\mathcal{T}_1})) + \\ & \sum_{\forall s \in \mathcal{S}_2} \log_2(1 + \hat{\gamma}_s^b(\psi_{tilt}^{\mathcal{T}_2})) + \\ & \sum_{\forall s \in \mathcal{S}_n} \log_2(1 + \hat{\gamma}_s^b(\psi_{tilt}^{\mathcal{T}_n})) + \dots \\ & + \sum_{\forall s \in \mathcal{S}_N} \log_2(1 + \hat{\gamma}_s^b(\psi_{tilt}^{\mathcal{T}_N})) \} \quad (28) \end{aligned}$$

where $N = |\mathcal{N}|$. According to (27) all the terms in the above series are in fact independent of each other, therefore the maximization can be performed on the individual terms of the series, so (28) can be written as:

$$\begin{aligned} \hat{\eta}_{max} = & \max_{\psi_{tilt}^{T_1}} \sum_{\forall s \in \mathcal{S}_1} \log_2 \left(1 + \hat{\gamma}_s^b \left(\psi_{tilt}^{T_1} \right) \right) + \\ & \max_{\psi_{tilt}^{T_2}} \sum_{\forall s \in \mathcal{S}_2} \log_2 \left(1 + \hat{\gamma}_s^b \left(\psi_{tilt}^{T_2} \right) \right) + \\ & \max_{\psi_{tilt}^{T_n}} \sum_{\forall s \in \mathcal{S}_n} \log_2 \left(1 + \hat{\gamma}_s^b \left(\psi_{tilt}^{T_n} \right) \right) + \dots \\ & + \max_{\psi_{tilt}^{T_N}} \sum_{\forall s \in \mathcal{S}_N} \log_2 \left(1 + \hat{\gamma}_s^b \left(\psi_{tilt}^{T_N} \right) \right) \quad (29) \end{aligned}$$

closing the summation gives following expression and thus proves the proposition

$$\max_{\psi_{tilt}^B} \hat{\zeta} = \sum_{\forall n \in \mathcal{N}} \left(\max_{\psi_{tilt}^{T_n}} \sum_{\forall s \in \mathcal{S}_n} \log_2 \left(1 + \hat{\gamma}_s^b \right) \right) \quad (30)$$

Referring back to the SO system of flocking birds, note that each bird adjusts its flight parameters with reference to the observation of only two adjacent birds. As a result the group flight efficiency optimal formation i.e. V-shape, is maintained only approximately, however a significant group-wide gain in flight efficiency is still achieved. Similarly, here the SIR $\hat{\gamma}_s^b \left(\psi_{tilt}^B \right)$ in (23) is based on interference perceived from two adjacent sectors only and therefore can achieve the objective in (21) only approximately (as shown through corollary 3) but significant system wide gain is possible as we will show in Section IV.

E. Solving the Local Subproblem

Based the arguments above, (24) can be solved by individually solving the N subproblems that appear in the summation in (30) as a small scale optimization problem over three tilt angles of the three most interfering adjacent cells only. This subproblem can be written as:

$$\hat{\zeta}_{n,max} = \max_{\psi_{tilt}^{T_n}} \sum_{\forall s \in \mathcal{S}_n} w_s \log_2 \left(1 + \hat{\gamma}_s^b \right) \quad (31)$$

Note that we have introduced a weight factor w_s to be associated with each cell CG in the triplet. This weight factor can be used to model the relative importance of each cell in a triplet, depending on the number of users in that cell, its size or its commercial significance and thus can capture certain aspects of the heterogeneity of the network at local scale.

The total achievable bandwidth normalized throughput at the CGs in an n^{th} triplet is given as:

$$\hat{\zeta}_n = w_1 \log_2 \left(1 + \hat{\gamma}_1^1 \right) + w_2 \log_2 \left(1 + \hat{\gamma}_2^2 \right) + w_3 \log_2 \left(1 + \hat{\gamma}_3^3 \right) \quad (32)$$

where postscripts denote sector and subscripts denote CG's within a given triplet as shown in figure 5. By substituting the value of $\hat{\gamma}_s^b$ from (23), (32) can be given by (33). In (33) we dropped the subscript n to indicate that the analysis presented

in sequel is valid for all triplets. The problem in (31) can be written in standard form:

$$\max_{\psi_{tilt}^1, \psi_{tilt}^2, \psi_{tilt}^3} \hat{\zeta} \left(\psi_{tilt}^1, \psi_{tilt}^2, \psi_{tilt}^3 \right) \quad (34)$$

subject to: $\psi_{tilt}^1, \psi_{tilt}^2, \psi_{tilt}^3 < 90^\circ$

As can be seen from the expanded form of the objective function of (34) in (33), and as we will observe in next section, (34) is a non convex optimization problem. However, notice that compared to (12), the problem in (34) is now a very small scale and much simpler optimization problem. This is because the number of optimization variables is only three compared to $|\mathcal{B}|$ and the summation in the optimization objective has only three terms, each with small constant evaluation complexity compared to $|\mathcal{R}| + |\mathcal{U} \setminus \mathcal{U}|$ terms in (12) each with evaluation complexity growing with $|\mathcal{B}|$. Note that the optimization parameters in (34) are confined to a finite range as $0^\circ < \psi < 90^\circ$. Since, practically a tilt accuracy of up to 1° is significant, the total search space of the optimization problem in (34) is limited to maximum of $90 \times 90 \times 90 = 729000$. Given a reasonably small fixed search space, any exhaustive search based heuristic can now be used to quickly solve (34) with an increased guarantee of quality of the solution compared to the original large scale problem. Or, alternatively, a solution can also be determined using nonlinear optimization technique that can tackle a small scale non-convex optimization objective. For example, noticing that the objective function is twice differentiable and the constraint is differentiable we can solve (34) using Sequential Quadratic Programming (SQP). To this end, the problem can be written in standard form as:

$$\min_{\psi} -\hat{\zeta}(\psi) \quad (35)$$

subject to: $g_j(\psi_j) < 0, j = 1, 2, 3$ where $\psi = [\psi_1, \psi_2, \psi_3]$ and $g_j(\psi_j) = \psi_j - 90$. Lagrangian of (35) can be given as:

$$\mathcal{L}(\psi, \lambda) = \hat{\zeta}(\psi) - \sum_{j=1}^3 \lambda_j (\psi_j - 90) \quad (36)$$

If $\hat{\mathbf{H}}$ denotes the approximate of the Hessian matrix \mathbf{H} , then we can define a quadratic subproblem to be solved at i^{th} iteration of SQP as follows:

$$\min_{\mathbf{w} \in \mathbb{R}^J} \frac{1}{2} \mathbf{w}^T \hat{\mathbf{H}} (\mathcal{L}(\psi, \lambda))_i \mathbf{w} + \nabla \hat{\zeta}(\psi)_i \mathbf{w} \quad (37)$$

subject to: $w_j + \psi_{j_i} - 90 < 0, j = 1, 2, 3$

Below we briefly describe the three main steps to solve the above problem through SQP

- 1) **Updating $\hat{\mathbf{H}}$:** At each iteration the value of $\hat{\mathbf{H}}$ is updated using the Broyden-Fletcher -Goldfarb -Shanno (BFGS) approximation method i.e.

$$\hat{\mathbf{H}}_{i+1} = \hat{\mathbf{H}}_i + \frac{\mathbf{b}_i \mathbf{b}_i^T}{\mathbf{b}_i^T \mathbf{a}_i} - \frac{\hat{\mathbf{H}}_i^T \mathbf{a}_i^T \mathbf{a}_i \hat{\mathbf{H}}_i}{\mathbf{a}_i^T \hat{\mathbf{H}}_i \mathbf{a}_i}$$

$$\hat{\zeta} = w_1 \log_2 \left(1 + \left(\frac{h_1^1 10^{-1.2\mu} ((\psi_1^1 - \psi_{i1t}^1)^2 + c_1^1)}{\left(h_1^2 10^{-1.2\mu} ((\psi_1^2 - \psi_{i1t}^2)^2 + c_1^2) \right) + \left(h_1^3 10^{-1.2\mu} ((\psi_1^3 - \psi_{i1t}^3)^2 + c_1^3) \right)} \right) \right) +$$

$$w_2 \log_2 \left(1 + \left(\frac{h_2^2 10^{-1.2\mu} ((\psi_2^2 - \psi_{i2t}^2)^2 + c_2^2)}{\left(h_2^1 10^{-1.2\mu} ((\psi_2^1 - \psi_{i2t}^1)^2 + c_2^1) \right) + \left(h_2^3 10^{-1.2\mu} ((\psi_2^3 - \psi_{i2t}^3)^2 + c_2^3) \right)} \right) \right) +$$

$$w_3 \log_2 \left(1 + \left(\frac{h_3^3 10^{-1.2\mu} ((\psi_3^3 - \psi_{i3t}^3)^2 + c_3^3)}{\left(h_3^1 10^{-1.2\mu} ((\psi_3^1 - \psi_{i3t}^1)^2 + c_3^1) \right) + \left(h_3^2 10^{-1.2\mu} ((\psi_3^2 - \psi_{i3t}^2)^2 + c_3^2) \right)} \right) \right) \quad (33)$$

where $a_i = \psi_{i+1} - \psi_i$ and

$$\mathbf{b}_i = \left(\nabla \hat{\zeta}(\boldsymbol{\psi})_{(i+1)} - \sum_{j=1}^3 \lambda_j \nabla g_{j,(i+1)} \right) - \left(\nabla \hat{\zeta}(\boldsymbol{\psi})_{(i)} - \sum_{j=1}^3 \lambda_j \nabla g_{j,(i)} \right) \quad (39)$$

- 2) **Solution of Quadratic subproblem:** Once the Hessian is known the problem in (37) is a quadratic programming problem that can be solved using standard methods. We use the gradient projection method as described in [37].
- 3) **Line search and Merit function** The solution of the quadratic subproblem in the i^{th} iteration of SQP algorithm returns the vector \mathbf{w}_i that provides the locus for the next iteration as $\boldsymbol{\psi}_{i+1} = \boldsymbol{\psi}_i + \rho \mathbf{w}_i$ where ρ is a set such that sufficient decrease in the merit function is achieved. We use the merit function defined in [38] i.e. given as

$$\varphi(\boldsymbol{\psi}) = \hat{\zeta}(\boldsymbol{\psi}) + \sum_{j=1}^3 \mu_j \cdot \max(0, g_j(\boldsymbol{\psi}_j)) \quad (40)$$

where μ is the penalty parameter which we set as recommended in [38] i.e.,

$$\mu_{j,(i)} = \mu_{j,(i+1)} = \max \left\{ \lambda_j, \frac{\mu_{j,(i)} + \lambda_j}{2} \right\}, j = 1, 2, 3 \quad (41)$$

Through the above steps of SQP, the problem in (34) can be solved within each triplet independently to determine the optimal tilt angles to be maintained by each of the three cells in the triplet for given locations of CG's within that triplet. The execution of these local solutions in each triplet in the cellular system locally results in the achievement of the system wide goal in (21) approximately, that in turn manifests the original system-wide objective in (12). Thus the optimal tilt angles can be maintained by dynamically responding to variations in the cellular system environment in a distributed manner to maintain enhanced spectral efficiency on the BS-RS links as well as on the BS-user links. In the following, we refer to this proposed solution as SOT (Self Organization of Tilts).

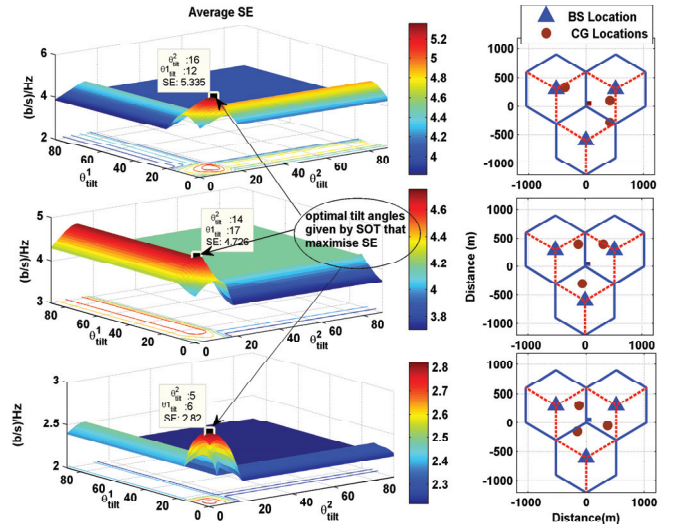


Fig. 6. $\hat{\zeta}$ plotted for a stand alone triplet against tilts of two sectors while third is fixed at 0° for three different CG locations within the triplet. It can be seen that optimal tilt angles for maximum spectral efficiency change as locations of CGs change.

IV. PERFORMANCE EVALUATION

In this section first we present the numerical results for SOT that are readily obtainable from the analysis presented above. This is followed by performance results of SOT evaluated by implementing SOT in a full scale system level simulator.

A. Numerical Results

1) **Analysing Robustness of SOT:** In this subsection we analyse the sensitivity of SOT's gain to varying locations of CG and also to two key design parameters i.e. antenna height and vertical antenna beam width. The objective of analysing SOT's gain sensitivity to these three factors is to investigate its robustness against randomness of user and BS relative locations, variety of BS heights and antenna types in real heterogeneous network. Numerical results for three random set of locations of CG's are plotted in figure 6. These results can be obtained by plotting (33) with $\beta = 4$, $B_v = 10^\circ$, $B_h = 70^\circ$ and cell radius of 600m, BS and CG height of 20m and 10m respectively; and by normalising $\hat{\zeta}$ by 3 i.e. the number of cells in the triplet. $\frac{\hat{\zeta}}{3}$ thus plotted in figure 6 gives the average spectral efficiency in a triplet. It can be seen that the adaptation

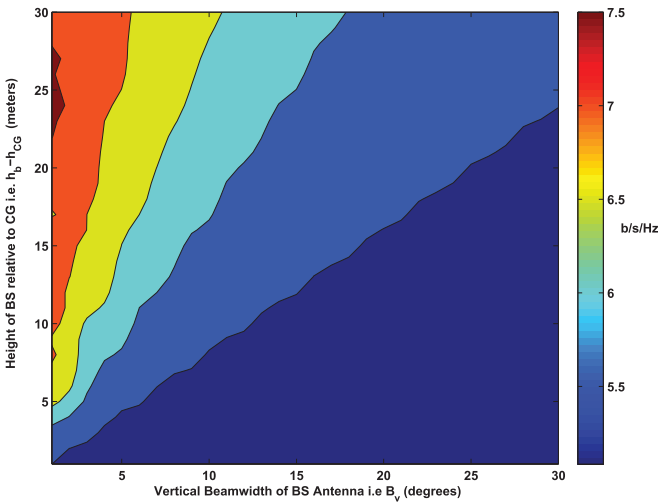


Fig. 7. Maximum spectral efficiency yielded by SOT for a given location CG's in triplet plotted for range of BS height above CG, and vertical beamwidth of antenna.

of antenna tilts can change the average spectral efficiency from 3.9 to 5.3, 3.7 to 4.7 and 2.1 to 2.8 b/s/Hz (from top to bottom respectively), depending on the location of CGs that represent either the RS or focal points of user distribution. Since SOT can dynamically determine the optimal tilt angles for any given locations of CGs in a triplet, it can self-optimize antenna tilts to maintain maximum spectral efficiency. In figure 6, the values of spectral efficiency achieved by optimal tilts determined through SOT can be compared to the spectral efficiency achievable with a wide range of other tilts. These results imply that SOT can yield a substantial gain in spectral efficiency compared to arbitrary tilting. However, the exact gain achievable by SOT is dependent on CG location and thus user distribution or RS location. It can be noticed from the contour plots in figure 6 that the optimal tilt angles generally lie in a much smaller range e.g this range is just $0^{\circ} - 20^{\circ}$ for the given cell radius and BS and RS heights. This observation can be used to further reduce the effective search space to only $20 \times 20 \times 20 = 8000$ combinations of tilt angles in a triplet to quickly determine the optimal tilt angles for any set of CG locations.

The gain SOT can yield is also dependent on the vertical beamwidth of the antenna and the relative height of the BS compared to the height of the CG. Figure 7 plots the maximum spectral efficiency SOT yields for a range of vertical beamwidth and height of the BS above the height of CG, for the locations of CG in the top right of figure 6. Results show that maximum achievable spectral efficiency by SOT can be further increased as the height of the antenna increases or the vertical beamwidth decreases. A high antenna allows the front lobe of the antenna to be focused more precisely on the CGs as can be seen in figure 4. A narrow beamwidth on the other hand allows the antenna tilt to play a stronger role in boosting the desired signal and attenuating the interference. Thus a decrease in vertical beamwidth and increase in antenna height both result in higher SIR and thus higher spectral efficiency.

2) *Comparing SOT with a Centralized Optimal Solution:* While the numerical results above demonstrate that SOT can

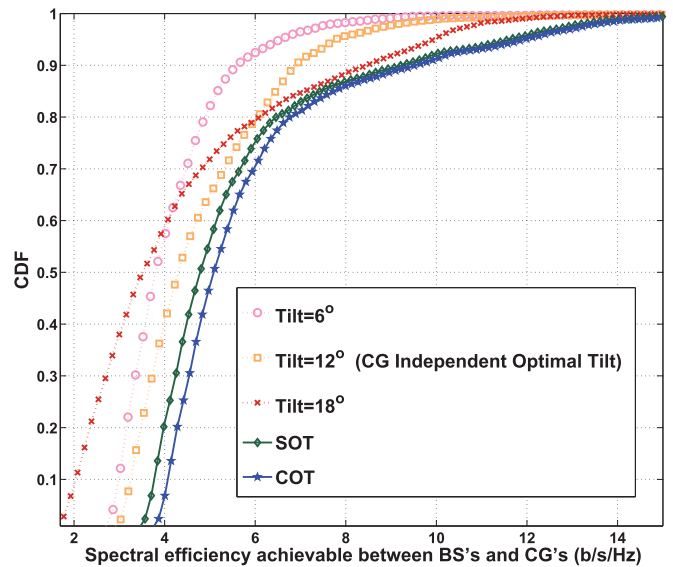


Fig. 8. SOT is compared with fixed tilting as well as Centralized Optimization of Tilts (COT). COT solution is obtained by solving (21) via brute force.

yield substantial gain for all possible CG locations and range of system design parameters, it is of interest to assess how far this gain is from that achievable by a hypothetical optimal solution that can perform a Centralized Optimization of Tilts (COT). Unlike, SOT that has a fixed search space of 90^3 and thus can be solved easily, COT will require joint optimization of system-wide antenna tilts and thus will have a search space of 90^B .

The COT solution is obtained by solving (21) through brute force for $7 \times 3 = 21$ cells. Note that a cross-comparison with heuristic based solutions is omitted not only because of unavailability of an exact work in the literature that considers a relay enhanced cellular system, but also because the outputs of such solutions are largely dependent on the configuration of the underlying heuristics making a meaningful comparison difficult. On the contrary, the chosen benchmarks are easily repeatable allowing a fair cross-comparison. They allow us to assess: 1) how much gain our solution yields compared to current commercially used pragmatic solutions; and 2) how far our distributed solution is from a hypothetical system-wide centralized absolutely optimal SO solution. Due to the computational time constraint for COT, only a tilt range of $6^{\circ} - 18^{\circ}$ is considered with a resolution of 2° . The rationale behind selecting this range is that it is centered around 12° . If we consider the centroid of the cell to be the CG, which will be the case when user distribution is perfectly uniform as explained above, the fixed optimal tilt for a given BS height of 32m, user height of 1.5m and intersite distance of 500m (see Table I) is 12° , i.e. $\arctan((32 - 1.5) / (\frac{500}{2\cos(30^{\circ})})) \approx 12^{\circ}$. Thus 6^{21} evaluations of the objective function in (21) are traversed to find the optimal solution. On a regular desktop computer (2.8 GHz processor, 8GB RAM) it took well over 8 hours. For fair comparison, SOT is also implemented under the same set up of tilt range, resolution and number of cells in the system.

Figure 8 plots the CDF of spectral efficiency achievable on links assumed between CGs and BS, with SOT and COT.

Note that albeit relying on local information only, SOT's performance is considerably close to COT. As expected, being globally optimal, COT does outperform SOT slightly. However, note that from a real world implementation point of view COT is difficult to implement not only because of the tremendous computation effort required but also due to the global signalling needed for its implementation (see Section V). The performance projected by COT in figure 8 does not take into account this large system wide signalling overhead. In terms of complexity, for even a cellular system as small as 19×3 cells (which is simulated for results in the next subsection), brute force based COT will have to do over 10^{99} evaluations of (21). Extrapolating the time of the conducted experiment, that may take years. However, despite its impracticality COT does serve the purpose of an upper bound to benchmark our solution. The small gap that SOT has from COT, is worth its distributed and system wide-signalling-free design that allows its computationally feasible solution and pragmatic implementation. In figure 8, the CDFs with a typical range of fixed tilting values are also plotted for comparison with fixed range tilting that is often empirically set in commercial cellular systems. It can be noted that SOT outperforms all fixed tilting schemes including the fixed optimal tilt of 12° . Reasons for this gain provided by SOT are explained in next subsection.

B. System Level Simulation Results

The numerical results presented above show the gain of SOT for BS-CG links only, while considering interference from a limited number of cells. As a real cellular system consists of a large number of cells, containing randomly located RS and users of different heights and antenna gains, these factors will affect the system level performance of SOT. In order to evaluate the performance of SOT in more realistic scenarios, in this subsection we present results obtained by implementing SOT in a full scale system level simulator. Key modelling parameters used in system level performance evaluation are 3GPP compliant and are listed in Table I. Our system level simulator models an OFDMA based generic cellular system where half of the cells contain randomly located RS and the other half, selected randomly, do not have RSs and are served by the BS only. Due to space limitations we present results for capacity enhancing RS only, as only in this case, does the backhaul optimization become significant. To model the capacity enhancing RS scenario, we assume that in the cells with RSs, 80% of the users in that cell are concentrated within 200m radius of the RS. In cells without RSs, users are randomly distributed across the cell. The simulator, is snapshot based and results reported are averaged over 10 snapshots of user and RS locations and tilt settings obtained via SOT for these user and RS distributions. Again comparison with prior works on heuristic based dynamic tilting schemes is omitted because of the reasons explained above. Instead, for the sake of reproducible performance evaluation, we compare the performance of SOT against a range of typical fixed antenna tilts including the fixed optimal tilt i.e. $0^\circ, 6^\circ, 12^\circ, 18^\circ$. Performance is evaluated for both BS-RS access links as well as BS-user coverage links.

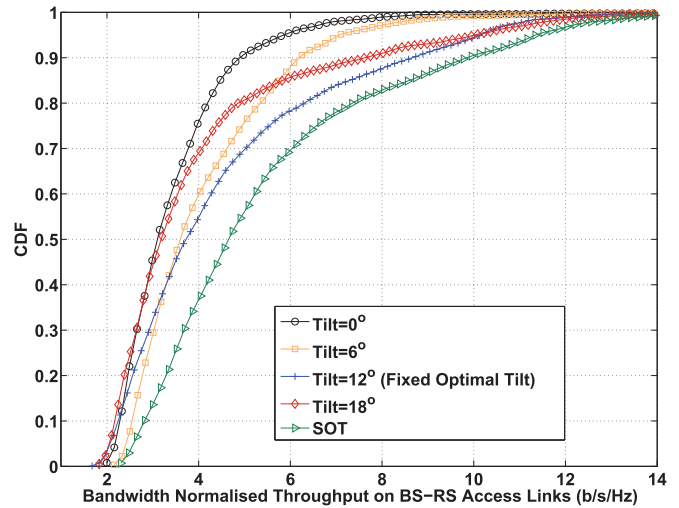


Fig. 9. CDF of spectral efficiency achievable on the BS-RS links with SOT and with classic fixed antenna tilts.

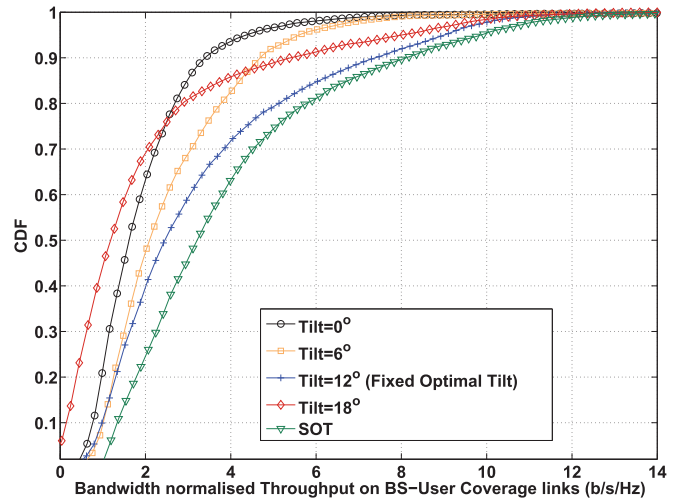


Fig. 10. CDF of spectral efficiency achievable on the BS-users links with SOT and with classic fixed antenna tilts.

Figure 9 plots the CDF of spectral efficiency achieved on the BS-RS access links. With $Tilt = 0^\circ$ performance is worse obviously due to high interference. With medium tilts of $Tilt = 6^\circ, 12^\circ$ spectral efficiency improves as interference in general decreases for all BS-RS links. As the tilts are further increased i.e. $Tilt = 18^\circ$ the spectral efficiency on the access links of RS that are located close to BS (50%-tile and above) improves due to reduced interference and increased antenna gain focused on them. However, the spectral efficiency of access links of RSs located at the cell edges (around 5%-tile and above) starts worsening, thereby nullifying the net gain in system wide average spectral efficiency. SOT, on the other hand provides a substantial net gain in spectral efficiency compared to all other fixed tilting options by dynamically setting tilts with respect to RS and CG locations.

Figure 10 plots the CDF of spectral efficiency achievable on BS-user links. The trends are the same as observed for RS-BS links except that, in general the spectral efficiency on BS-user links is lower than that on access links. This is due to the different pathloss models on the two types of links i.e. BS-RS has much less shadowing than BS-user links.

TABLE I
3GPP COMPLIANT SYSTEM LEVEL SIMULATION PARAMETERS [39]

Parameters	Values
System topology	19 BS with 3 sector/cells per BS
BS Transmission Power	46 dBm
BS Inter site distance	500 meters
BS height	32 meters
RS height	5m
RS Type	Capacity Extension i.e. $w_r = 1, \forall r \in R$
User height	1.5 meters
User activity levels	$a_u = 1, \forall u \in U$
Network Topology Type	Homogenous, $w_s = 1, \forall s \in S$
User antenna	5 dB (Omni directional)
RS antenna	7 dB (Omni directional)
BS antenna horizontal beamwidth, B_h	70^0
BS antenna vertical beamwidth, B_v	10^0
BS antenna vertical Gain Weight, λ_v	0.5
BS antenna vertical Gain Weight, λ_h	0.5
BS antenna maximum gain, G_{max}	14 dB
BS antenna maximum attenuation, A_{max}	25 dB
Frequency	2 GHz
Pathloss model	Urban, Scenario 1 [39]
Shadowing standard deviation on BS-user links	8 dB
Shadowing standard deviation on BS-RS links	4 dB

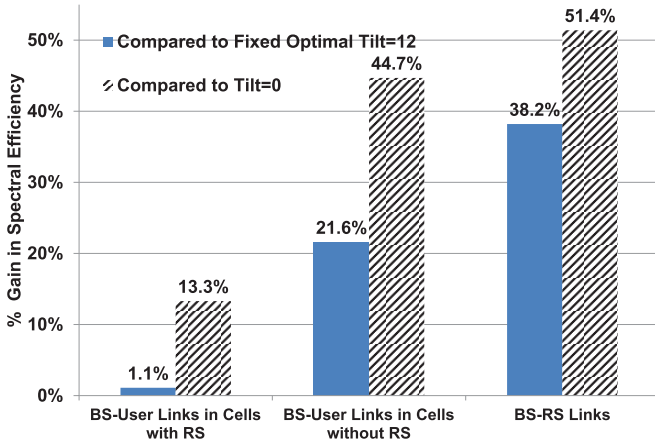


Fig. 11. Average spectral efficiency with SOT and with fixed tilts on BS-RS and BS-user links.

Furthermore, unlike RS that can be perfectly represented by one point in a cell used as CG in SOT, users are distributed all over the cells. Therefore, optimizing antenna tilts with respect to a single point that represent all users in cells (i.e. CG), is effective but not as much as it is for RS. For the same reason, high values of fixed tilts i.e. $Tilt = 18^0$ has more adverse effect on BS-user links, than it has on BS-RS links as the large tilt can particularly cause outage for the cell edge users. The exact percentage of such outage may depend on the antenna and transmission parameters and cell size. Nevertheless, it can be seen that SOT yields a net gain in spectral efficiency compared to fixed tilting on BS-user links as well, as it intelligently sets tilt values based on user concentrations.

A more quantitative perspective of the gain in spectral efficiency SOT can give on BS-RS and BS-user links, is presented in figure 11 that plots the percentage gain in average spectral efficiency SOT yielded when compared to the fixed optimal tilt of 12^0 and no tilting at all. It can be observed that for the cells with RS, BS-user links of the 20% users that are not explicitly considered by SOT while determining tilt, no significant gain is achieved compared to fixed optimal tilt, as expected. However, for rest of the users, as well as, RSs

that are considered in determining the CGs, SOT yields very substantial gains compared to fixed tilting.

V. PRACTICAL IMPLEMENTATION OF SOT

In this paper we demonstrated the gain of the proposed framework mainly in context of a hexagonal grid model only, for tractability and brevity reasons. However, SOT is implementable in a real heterogeneous network as long as the network topology allows decomposition into local non-overlapping cluster of cells (e.g. quartet, quintet, sextuplet) with the same property as a triplet i.e. a set of most interfering cells that can be repeated to cover the whole network without overlap. The weight factors incorporated into the framework while calculating CGs can actually be used to take into account other types of heterogeneity such as cell sizes, sector spreads and azimuth angle biases, other than user profiling and RS types. Though the exact gain of SOT will vary depending on actual system parameters and topology as pointed out via results in section IV-A1, the key advantage of SOT is that it is practically implementable even with state of the art technologies. Since the proposed framework does not incur heavy signaling overheads and has very low implementation complexity and cost, even reduced gain due to the irregularity of grid and propagation scattering is an added advantage compared to state of the art offline fixed empirical tilting. The RS and user positions information can be easily gathered at the respective BS with existing location estimation techniques such as GPS or the host of alternative cellular positioning techniques. For RS, the location update will be required only when the location of the RS changes. As far as need for user locations is concerned, as discussed earlier, as long as the user distribution and activity level can be assumed to be uniform, the CG lies at the centroid of the sector, and can be determined by system design parameters available offline, namely cell radius, antenna pattern and height. Thanks to the distributed nature of the solution, even for cells with highly dynamic non-uniform user distribution, when a tilt update is needed, CG calculation requires SINR perceived by each user along with its position, to be known only at the serving BS. Since the SINR indicator is already available to a BS in LTE in the form of CQI (for scheduling purposes), this

means negligible additional signalling is required to determine the CGs in each cell in an online manner. The existing X2 interface can be used to promptly exchange the CG locations, only among the three adjacent cells that make each triplet. Based on this CG information, the optimal tilt angle for all the three cells within each triplet in the system can be determined via SOT. In emerging cellular systems, BS tilts can be adjusted electronically, with the implementation of SOT BS's can autonomously and dynamically maintain their antenna tilts to cope with changes in the cellular eco system. Therefore, this algorithm requires no human intervention, thereby promising significant OPEX saving. Another advantage of SOT is that due to its highly localized nature it is very agile as it does not suffer from excessive delays. Therefore, SOT can be implemented in an online manner using event based triggering mechanisms. Such triggering mechanisms can detect 'turning on or off' of RSs or major variations in user demography, and thus can autonomously update the BS antenna tilts in the respective triplet(s) to maintain maximum spectral efficiency.

VI. CONCLUSIONS

An analytical framework for distributed Self Organization of BS Tilts, named SOT, has been presented. SOT can autonomously determine and set optimal tilts in order to maximize spectral efficiency on the BS-RS as well as BS-user links in a live heterogeneous network. Both numerical and simulation results show that a gain of 10-50% in spectral efficiency compared to typical fixed optimal tilting can be obtained with SOT depending on system topology and user demography. SOT yields this gain as it calculates and then dynamically adapts cell specific optimal tilt values by taking into account users' and RSs' locations and activity levels. SOT's comparison with a centralized tilt optimization solution—which is difficult to implement in a real network due to its excessive signaling overhead and computational complexity—shows, SOT can yield performance close to a centralized tilt optimization solution. The key advantage of SOT is that it implementable with state of art technology and relies only on local signaling. Therefore, it has potential for implementation to autonomously optimize antenna tilts in a live cellular network in order to cope with either ever changing user demography or the impromptu deployment of new RSs.

ACKNOWLEDGMENT

This work was made possible by NPRP grant No. 5 - 1047 - 2 437 from the Qatar National Research Fund (a member of The Qatar Foundation). Authors would like to thank the anonymous reviewers, Mr. Colin O'Reily and Mr. Bernard Hunt for providing extremely helpful reviews.

REFERENCES

- [1] M. Dohler, R. Heath, A. Lozano, C. Papadias, and R. Valenzuela, "Is the PHY layer dead?" *IEEE Commun. Mag.*, vol. 49, no. 4, pp. 159–165, Apr. 2011.
- [2] A. Imran and R. Tafazolli, "Evaluation and comparison of capacities and costs of multihop cellular networks," in *Proc. 2009 International Conference on Telecommunications*, pp. 160–165. Available: <http://portal.acm.org/citation.cfm?id=1700234.1700264>
- [3] K. Jacobson and W. Krzymien, "System design and throughput analysis for multihop relaying in cellular systems," *IEEE Trans. Veh. Technol.*, vol. 58, no. 8, pp. 4514–4528, Oct. 2009.
- [4] 3GPP, "Self-organising networks; concepts and requirements," 3GPP TS 32.500 v10.1.0, Tech. Rep., 2010.
- [5] S. Xu and Y. Hua, "Optimal design of spatial source-and-relay matrices for a non-regenerative two-way MIMO relay system," *IEEE Trans. Wireless Commun.*, vol. 10, no. 5, pp. 1645–1655, May 2011.
- [6] O. Oyman, "Opportunistic scheduling and spectrum reuse in relay-based cellular networks," *IEEE Trans. Wireless Commun.*, vol. 9, no. 3, pp. 1074–1085, Mar. 2010.
- [7] R. Babaee and N. Beaulieu, "Cross-layer design for multihop wireless relaying networks," *IEEE Trans. Wireless Commun.*, vol. 9, no. 11, pp. 3522–3531, Nov. 2010.
- [8] E. Amaldi, A. Capone, and F. Malucelli, "Optimizing UMTS radio coverage via base station configuration," in *Proc. 2002 IEEE International Symposium on Personal, Indoor and Mobile Radio Communications*, vol. 1, pp. 315–319.
- [9] I. Siomina, P. Varbrand, and D. Yuan, "Automated optimization of service coverage and base station antenna configuration in UMTS networks," *IEEE Wireless Commun.*, vol. 13, no. 6, pp. 16–25, Dec. 2006.
- [10] F. Gunnarsson, M. Johansson, A. Furuskar, M. Lundevall, A. Simonsson, C. Tidestav, and M. Blomgren, "Downtilted base station antennas—a simulation model proposal and impact on HSPA and LTE performance," in *Proc. 2008 IEEE Vehicular Technology Conference – Fall*, pp. 1–5.
- [11] R. Pazhyannur, T. Dean, S. Anantha, and R. Dham, "RF optimization of WiMAX systems," in *Proc. 2008 IEEE Vehicular Technology Conference – Fall*, pp. 1–5.
- [12] O. N. Yilmaz, S. Hämäläinen, and J. Hämäläinen, "Comparison of remote electrical and mechanical antenna downtilt performance for 3GPP LTE," in *Proc. 2009 IEEE Vehicular Technology Conf. – Fall*, pp. 1–5.
- [13] R. Abou-Jaoude, N. Ulhaq, and C. Hartmann, "HSDPA throughput optimization with antenna tilt and pilot power in a moving hot-spot scenario," in *Proc. 2009 IEEE Vehicular Technology Conference – Fall*, pp. 1–5.
- [14] M. N. ul Islam, R. Abou-Jaoude, C. Hartmann, and A. Mitschele-Thiel, "Self-optimization of antenna tilt and pilot power for dedicated channels," in *Proc. 2010 International Symposium on Modeling and Optimization in Mobile, Ad Hoc and Wireless Networks*, pp. 196–203.
- [15] R. Razavi, S. Klein, and H. Claussen, "Self-optimization of capacity and coverage in LTE networks using a fuzzy reinforcement learning approach," in *Proc. 2010 IEEE Int. Personal Indoor and Mobile Radio Communications Symp.*, pp. 1865–1870.
- [16] O. N. Yilmaz, J. Hämäläinen, and S. Hämäläinen, "Self-optimization of remote electrical tilt," in *Proc. 2010 IEEE International Symposium on Personal Indoor and Mobile Radio Communications*, pp. 1128–1132.
- [17] —, "Optimization of adaptive antenna system parameters in self-organizing LTE networks," *Wireless Networks*, pp. 1–17, 2012. Available: <http://dx.doi.org/10.1007/s11276-012-0531-3>
- [18] M. Amirijoo, L. Jorgueski, R. Litjens, and R. Nascimento, "Effectiveness of cell outage compensation in LTE networks," in *Proc. 2011 IEEE Consumer Communications and Networking Conference*, pp. 642–647.
- [19] H. Eckhardt, S. Klein, and M. Gruber, "Vertical antenna tilt optimization for LTE base stations," in *Proc. 2011 IEEE Vehicular Technology Conference – Spring*, pp. 1–5.
- [20] A. Awada, B. Wegmann, I. Viering, and A. Klein, "Optimizing the radio network parameters of the long term evolution system using Taguchi's method," *IEEE Trans. Veh. Technol.*, vol. 60, no. 8, pp. 3825–3839, Oct. 2011.
- [21] H. Klessig, A. Fehske, G. Fettweis, and J. Voigt, "Improving coverage and load conditions through joint adaptation of antenna tilts and cell selection rules in mobile networks," in *Proc. 2012 International Symposium on Wireless Communication Systems*, pp. 21–25.
- [22] N. Seifi, M. Coldrey, and M. Viberg, "Throughput optimization for MISO interference channels via coordinated user-specific tilting," *IEEE Commun. Lett.*, vol. 16, no. 8, pp. 1248–1251, Aug. 2012.
- [23] M. Naseer ul Islam and A. Mitschele-Thiel, "Cooperative fuzzy Q-Learning for self-organized coverage and capacity optimization," in *Proc. 2012 IEEE International Symposium on Personal Indoor and Mobile Radio Communications*, pp. 1406–1411.
- [24] W. Luo, J. Zeng, X. Su, J. Li, and L. Xiao, "A mathematical model for joint optimization of coverage and capacity in self-organizing network in centralized manner," in *Proc. 2012 International ICST Conference on Communications and Networking in China*, pp. 622–626.
- [25] A. Thampi, D. Kaleshi, P. Randall, W. Featherstone, and S. Armour, "A sparse sampling algorithm for self-optimisation of coverage in

- LTE networks,” in *Proc. 2012 International Symposium on Wireless Communication Systems*, pp. 909–913.
- [26] S. Hurley, S. Allen, D. Ryan, and R. Taplin, “Modelling and planning fixed wireless networks,” *Wirel. Netw.*, vol. 16, no. 3, pp. 577–592, Apr. 2010. Available: <http://dx.doi.org/10.1007/s11276-008-0155-9>
- [27] O. Aliu, A. Imran, M. Imran, and B. Evans, “A survey of self organisation in future cellular networks,” *IEEE Commun. Surveys Tutorials*, vol. PP, no. 99, pp. 1–26, 2012.
- [28] R. Razavi, “Self-optimisation of antenna beam tilting in lte networks,” in *Proc. 2012 IEEE Vehicular Technology Conference – Spring*, pp. 1–5.
- [29] A. Imran, M. Imran, and R. Tafazolli, “Relay station access link spectral efficiency optimization through SO of macro BS tilts,” *IEEE Commun. Lett.*, vol. 15, pp. 1326–1328, 2011.
- [30] X. Yang and R. Tafazolli, “A method of generating cross-correlated shadowing for dynamic system-level simulators,” in *Proc. 2003 Personal, Indoor and Mobile Radio Communications*, vol. 1, pp. 638–642.
- [31] I. Viering, M. Döttling, and A. Lobinger, “A mathematical perspective of self-optimizing wireless networks,” *Proc. 2009 IEEE International Conference on Communications*, pp. 1–6.
- [32] C. Prehofer and C. Bettstetter, “Self-organization in communication networks: principles and design paradigms,” *IEEE Commun. Mag.*, vol. 43, no. 7, pp. 78–85, July 2005.
- [33] A. Imran, M. Bennis, and L. Giupponi, “Use of learning, game theory and optimization as biomimetic approaches for self-organization in macro-femtocell coexistence,” in *Proc. 2012 IEEE Wireless Communications and Networking Conference*, pp. 103–108.
- [34] T. Jansen, M. Amirijoo, U. Turke, L. Jorgueski, K. Zetterberg, R. Nascimento, L. Schmelz, J. Turk, and I. Balan, “Embedding multiple self-organisation functionalities in future radio access networks,” in *Proc. 2009 IEEE Vehicular Technology Conference – Spring*, pp. 1–5.
- [35] S. Hämäläinen, H. Sanneck, and C. Sartori, Eds., *LTE Self-Organizing Networks (SON): Network Management Automation for Operational Efficiency*. Wiley, 2012.
- [36] P. B. S. Lissaman and C. A. Shollenberger, “Formation flight of birds,” *Science*, vol. 168, no. 3934, pp. 1003–1005, 1970. Available: <http://www.sciencemag.org/cgi/content/abstract/168/3934/1003>
- [37] P. Gill, W. Murray, and M. H. Wright, *Practical Optimization*. Academic Press, 1981.
- [38] M. Powell, “A fast algorithm for nonlinearly constrained optimization calculations,” in *Numerical Analysis*, ser. Lecture Notes in Mathematics, G. Watson, Ed. Springer Berlin / Heidelberg, 1978, vol. 630, pp. 144–157, 10.1007/BFb0067703. Available: <http://dx.doi.org/10.1007/BFb0067703>
- [39] A. B. Saleh, S. Redana, J. Hämäläinen, and B. Raaf, “On the coverage extension and capacity enhancement of inband relay deployments in lte-advanced networks,” *JECE*, vol. 2010, pp. 4:1–4:10, Jan. 2010. Available: <http://dx.doi.org/10.1155/2010/894846>



Ali Imran is an assistant professor in telecommunications at University of Oklahoma, since Jan 2014. From, Oct-2011 to Jan-2014, he worked as a research scientist at QMIC, Doha, Qatar (www.qmic.com). In that position, he conducted research on a wide range of innovative solutions by drawing mainly on disciplines of telecommunications, software development and sensor networks. He is also leading a multinational \$1.045 million research project on Self Organizing Wireless Networks, QSON (www.qson.org). Before joining

QMIC in Oct-2011, since Oct-2007, he was a research fellow (part time and then full time) in wireless systems at Centre for Communication Systems Research, (CCSR) University of Surrey, UK. In that position Dr. Imran has contributed to a number of pan-European and international research projects while working in close collaboration with key industrial players such as NEC Europe Ltd. (UK), Telefonica (Spain), DOCOMO (Germany), Polska Telefonia Cyfrowa (Poland), Qualcomm (Germany), TTI (Spain), mimoOn (Germany), CTTC (Spain), CEA- LETI (France). There he also taught a number of courses and supervised graduate research students. From March 2002, till Oct-2007 he has worked as a communication lab instructor, BS deployment team leader and RF consultant to a leading telecom company in Pakistan. His research interest include, self-organizing networks, radio resource management and participatory sensing. He has authored over 25 peer reviewed journal and conference papers, two book chapters and a patent. He has presented number of tutorials at international forums such as IEEE ICC and WCNC. He is an Associate Fellow of Higher Education Academy (AFHEA), UK



Muhammad Ali Imran (M’03, SM’12) received his M.Sc. (Distinction) and Ph.D. degrees from Imperial College London, UK, in 2002 and 2007, respectively. He is currently a Reader in the Centre for Communication Systems Research (CCSR) at the University of Surrey, UK. In this role, he is leading a number of multimillion international research projects encompassing the areas of energy efficiency, fundamental performance limits, sensor networks and self-organizing cellular networks. He is leading the new physical layer work area under a large grant of above 35m for a 5G innovation center and an outdoor cellular test bed in CCSR, Surrey. He has a global collaborative research network spanning both academia and key industrial players in the field of wireless communications. He has supervised 16 successful Ph.D. graduates and published over 150 peer-reviewed research papers including more than 20 IEEE Journals. His research interests include the derivation of information theoretic performance limits, energy efficient design of cellular system and learning/self-organizing techniques for optimization of cellular system operation.



Adnan Abu-Dayya has more than 25 years of global experience in the areas of ICT R&D, product innovations, business development, and services delivery. Before moving to Qatar in 2007, he worked for 10 years at AT&T Wireless in Seattle, USA where he served in a number of management positions covering product innovations, emerging technologies, systems engineering, and IP Management and Licensing. Before that, Adnan worked as a Manager at Nortel Networks and as a Senior Consultant at the Communications Research Centre in Ottawa,

Canada. From April 2007 to Dec. 2008, he was the Chairman of the Electrical Engineering Department at Qatar University. He led the initiative to create and then was appointed as the Founding Executive Director (CEO) of the Qatar Mobility Innovations Center (QMIC) in 2009 at the Qatar Science & Technology Park, Qatar. Adnan received his Ph.D. in Electrical Engineering from Queens University, Canada in 1992. He has many issued patents and more than sixty publications. Dr. Abu-Dayya serves on the advisory boards of the Arab Innovation Network, and the Department of Electrical and Computer Engineer at Texas A&M University at Qatar.



Rahim Tafazolli is the Director of the Centre for Communications Systems Research (CCSR), Faculty of Engineering and Physical Sciences, The University of Surrey in the UK. He has published more than 500 research papers in refereed journals, international conferences and as invited speaker. He currently has more than 20 patents in the field of mobile communications. He is the editor of two books on *Technologies for Wireless Future* published by Wiley’s Vol.1 in 2004 and Vol.2 2006. He is currently chairman of EU Net!Works Technology

Platform Expert Group. He is Fellow of IET, WWRP (Wireless World Research Forum) and a Senior member of IEEE.

APPENDIX A

In order to prove theorem 1 we need to show that:

$$\sum_{\forall u \in \mathcal{U}_b} a_u \log_2(1 + \tilde{\gamma}_u^b(\tilde{\psi}_{tilt}^b)) = \max_{\psi_{tilt}^b} \sum_{\forall u \in \mathcal{U}_b} a_u \log_2(1 + \gamma_u^b(\psi_{tilt}^b)) \quad (42)$$

if

$$\int_x \int_y a_{(x,y)} \left((\psi_{x,y}^b - \tilde{\psi}_{tilt}^b) \frac{\tilde{\gamma}_{x,y}^b}{1 + \tilde{\gamma}_{x,y}^b} \right) dx dy = 0 \quad (43)$$

where \mathcal{U}_b is the set of user locations in the b^{th} cell such that $\mathcal{U}_b \subset \mathcal{U}$. Let $\tilde{\gamma}_u^b$ be the SIR in the b^{th} sector at u^{th} point, with optimal antenna tilt given as:

$$\tilde{\gamma}_u^b = \frac{d_u^{b-\beta} 10^{-1.2 \left(\lambda_v \left(\frac{\psi_u^b - \tilde{\psi}_{tilt}^b}{B_v} \right)^2 + \lambda_h \left(\frac{\phi_u^b - \phi_{tilt}^b}{B_h} \right)^2 \right)}}{\sum_{\forall b \in \mathcal{B} \setminus b} \left(d_u^{b-\beta} 10^{-1.2 \left(\lambda_v \left(\frac{\psi_u^b - \tilde{\psi}_{tilt}^b}{B_v} \right)^2 + \lambda_h \left(\frac{\phi_u^b - \phi_{tilt}^b}{B_h} \right)^2 \right)} \right)} \quad (44)$$

Let $\tilde{\psi}_{tilt}^b$ be the tilt that maximizes/minimizes the weighted sum throughput $\tilde{\zeta}^b$ in that cell, then

$$\frac{\partial \tilde{\zeta}^b}{\partial \tilde{\psi}_{tilt}^b} = \frac{\partial}{\partial \tilde{\psi}_{tilt}^b} \left(\sum_{u=1}^{|\mathcal{U}_b|} (a_u \log_2(1 + \tilde{\gamma}_u^b(\psi_{tilt}^b))) \right) = 0 \quad (45)$$

$$\frac{1}{\ln 2} \sum_{u=1}^{|\mathcal{U}_b|} a_u \left(\frac{\frac{\partial}{\partial \tilde{\psi}_{tilt}^b} \tilde{\gamma}_u^b(\psi_{tilt}^b)}{1 + \tilde{\gamma}_u^b(\psi_{tilt}^b)} \right) = 0 \quad (46)$$

$$\frac{\partial \tilde{\gamma}_u^b}{\partial \tilde{\psi}_{tilt}^b} = \frac{\frac{\partial}{\partial \tilde{\psi}_{tilt}^b} v}{\sum_{\forall b \in \mathcal{B} \setminus b} \left(d_u^{b-\beta} 10^{-1.2 \left(\lambda_v \left(\frac{\psi_u^b - \tilde{\psi}_{tilt}^b}{B_v} \right)^2 + \lambda_h \left(\frac{\phi_u^b - \phi_{tilt}^b}{B_h} \right)^2 \right)} \right)} \quad (47)$$

where

$$\frac{\partial}{\partial \tilde{\psi}_{tilt}^b} v = \frac{\partial}{\partial \tilde{\psi}_{tilt}^b} \left(d_u^{b-\beta} 10^{-1.2 \left(\lambda_v \left(\frac{\psi_u^b - \tilde{\psi}_{tilt}^b}{B_v} \right)^2 + \lambda_h \left(\frac{\phi_u^b - \phi_{tilt}^b}{B_h} \right)^2 \right)} \right) \quad (48)$$

$$= d_u^{b-\beta} 10^{-1.2 \left(\lambda_v \left(\frac{\psi_u^b - \tilde{\psi}_{tilt}^b}{B_v} \right)^2 + \lambda_h \left(\frac{\phi_u^b - \phi_{tilt}^b}{B_h} \right)^2 \right)} \ln 10 \frac{\partial}{\partial \tilde{\psi}_{tilt}^b} \left(-1.2 \left(\lambda_v \left(\frac{\psi_u^b - \tilde{\psi}_{tilt}^b}{B_v} \right)^2 + \lambda_h \left(\frac{\phi_u^b - \phi_{tilt}^b}{B_h} \right)^2 \right) \right) \quad (49)$$

$$= C (\psi_u^b - \tilde{\psi}_{tilt}^b) d_u^{b-\beta} 10^{-1.2 \left(\lambda_v \left(\frac{\psi_u^b - \tilde{\psi}_{tilt}^b}{B_v} \right)^2 + \lambda_h \left(\frac{\phi_u^b - \phi_{tilt}^b}{B_h} \right)^2 \right)} \quad (50)$$

where, $C = \frac{2.4 \ln 10 \lambda_v}{B_v^2}$. Putting v back in (47) and then using (47) in (46)

$$\frac{\partial \tilde{\zeta}^b}{\partial \tilde{\psi}_{tilt}^b} = \sum_{u=1}^{|\mathcal{U}_b|} a_u \left(\frac{C (\psi_u^b - \tilde{\psi}_{tilt}^b) d_u^{b-\beta} 10^{-1.2 \left(\lambda_v \left(\frac{\psi_u^b - \tilde{\psi}_{tilt}^b}{B_v} \right)^2 + \lambda_h \left(\frac{\phi_u^b - \phi_{tilt}^b}{B_h} \right)^2 \right)}}{\sum_{\forall b \in \mathcal{B} \setminus b} \left(d_u^{b-\beta} 10^{-1.2 \left(\lambda_v \left(\frac{\psi_u^b - \tilde{\psi}_{tilt}^b}{B_v} \right)^2 + \lambda_h \left(\frac{\phi_u^b - \phi_{tilt}^b}{B_h} \right)^2 \right)} \right)} \right) = 0 \quad (51)$$

Using (44) in (51)

$$\frac{\partial \tilde{\zeta}^b}{\partial \tilde{\psi}_{tilt}^b} = \sum_{u=1}^{|\mathcal{U}_b|} a_u \left((\psi_u^b - \tilde{\psi}_{tilt}^b) \frac{\tilde{\gamma}_u^b}{1 + \tilde{\gamma}_u^b} \right) = 0 \quad (52)$$

It can be shown easily that $\frac{\partial \partial \tilde{\zeta}^b}{\partial \partial \tilde{\psi}_{tilt}^b} < 0$, implying that the stationary point at $\tilde{\psi}_{tilt}^b$ is a maximum. If user distribution is uniform and u is substantially large, we can replace the summation in (52) with the surface integral over the whole area making it independent of individual user locations:

$$\int_x \int_y a_{(x,y)} \left((\psi_{x,y}^b - \tilde{\psi}_{tilt}^b) \frac{\tilde{\gamma}_{x,y}^b}{1 + \tilde{\gamma}_{x,y}^b} \right) dx dy = 0 \quad (53)$$

where $a_{(x,y)}$ is the weight associated with each point. Hence theorem 1.

APPENDIX B

Lemma 1 is quite intuitive and in order to prove it we actually need to show that

$$\gamma_s^b(\boldsymbol{\psi}_{\text{tilt}}^B) \leq \hat{\gamma}_s^b(\boldsymbol{\psi}_{\text{tilt}}^{\hat{B}}), \quad \forall s \in \mathcal{S} \tag{54}$$

$$\frac{h_p^b 10^{\mu((\psi_s^b - \psi_{\text{tilt}}^b)^2 + c_s^b)}}{\sum_{\forall \check{b} \in \mathcal{B} \setminus b} \left(h_s^b 10^{\mu((\psi_s^{\check{b}} - \psi_{\text{tilt}}^{\check{b}})^2 + c_k^{\check{b}})} \right)} \leq \frac{h_s^b 10^{\mu((\psi_s^b - \psi_{\text{tilt}}^b)^2 + c_s^b)}}{\sum_{\forall \check{b} \in \hat{\mathcal{B}} \setminus b} \left(h_p^{\check{b}} 10^{\mu((\psi_s^{\check{b}} - \psi_{\text{tilt}}^{\check{b}})^2 + c_s^{\check{b}})} \right)}, \forall s \in \mathcal{S} \tag{55}$$

Multiplying both sides by the inverse of the numerator and then inverting both sides

$$\sum_{\forall \check{b} \in \mathcal{B} \setminus b} \left(h_s^{\check{b}} 10^{\mu((\psi_s^{\check{b}} - \psi_{\text{tilt}}^{\check{b}})^2 + c_s^{\check{b}})} \right) \geq \sum_{\forall \check{b} \in \hat{\mathcal{B}} \setminus b} \left(h_s^{\check{b}} 10^{\mu((\psi_s^{\check{b}} - \psi_{\text{tilt}}^{\check{b}})^2 + c_s^{\check{b}})} \right), \forall s \in \mathcal{S} \tag{56}$$

By opening the left hand side

$$\begin{aligned} & \sum_{\forall \check{b} \in \hat{\mathcal{B}} \setminus b} \left(h_s^{\check{b}} 10^{\mu((\psi_s^{\check{b}} - \psi_{\text{tilt}}^{\check{b}})^2 + c_s^{\check{b}})} \right) + \sum_{\forall \check{b} \in \mathcal{B} \setminus \hat{\mathcal{B}}} \left(h_s^{\check{b}} 10^{\mu((\psi_s^{\check{b}} - \psi_{\text{tilt}}^{\check{b}})^2 + c_s^{\check{b}})} \right) \geq \\ & \sum_{\forall \check{b} \in \hat{\mathcal{B}} \setminus b} \left(h_s^{\check{b}} 10^{\mu((\psi_s^{\check{b}} - \psi_{\text{tilt}}^{\check{b}})^2 + c_s^{\check{b}})} \right) \\ & \text{since } \sum_{\forall \check{b} \in \mathcal{B} \setminus \hat{\mathcal{B}}} \left(h_s^{\check{b}} 10^{\mu((\psi_s^{\check{b}} - \psi_{\text{tilt}}^{\check{b}})^2 + c_s^{\check{b}})} \right) \geq 0 \end{aligned}$$

Hence the proposition in (54) is true. Since ζ is a monotonically increasing function of γ , $\gamma_s^b \leq \hat{\gamma}_s^b, \forall s \in \mathcal{S}$ implies that $\hat{\zeta} \geq \zeta$.